GSG2 knockdown suppresses cholangiocarcinoma progression by regulating cell proliferation, apoptosis and migration

JUN ZHOU[1], WANPIN NIE[2], JIAJIA YUAN[1], ZEYU ZHANG[2], LIANGLIANG MI[2], CHANGFA WANG[2] and RANGLANG HUANG[2]

[1]Peking University Cancer Hospital and Institute, Beijing 100142; [2]Department of Hepatobiliary and Pancreatic Surgery, The Third Xiangya Hospital of The Central South University, Changsha, Hunan 410013, P.R. China

Received August 31, 2020; Accepted March 18, 2021

DOI: 10.3892/or.2021.8042

Abstract. Cholangiocarcinoma (CCA) is the second most common type of hepatocellular carcinoma characterized by high aggressiveness and extremely poor patient prognosis. The germ cell-specific gene 2 protein (GSG2) is a histone H3 threonine-3 kinase required for normal mitosis. Nevertheless, the role and mechanism of GSG2 in the progression and development of CCA remain elusive. In the present study, the association between GSG2 and CCA was elucidated. Firstly, we demonstrated that GSG2 was overexpressed in CCA specimens and HCCC-9810 and QBC939 cells by immunohistochemical (IHC) staining. It was further revealed that high expression of GSG2 in CCA had significant clinical significance in predicting disease deterioration. Subsequently, cell proliferation, apoptosis, cell cycle distribution and migration were measured by MTT, flow cytometry, and wound healing assays, respectively *in vitro*. The results demonstrated that downregulation of GSG2 decreased proliferation, promoted apoptosis, arrested the cell cycle and weakened migration in the G2 phase of CCA cells. Additionally, GSG2 knockdown inhibited CCA cell migration by suppressing epithelial-mesenchymal transition (EMT)-related proteins, such as N-cadherin and vimentin. Mechanistically, GSG2 exerted effects on CCA cells by modulating the PI3K/Akt, CCND1/CDK6 and MAPK9 signaling pathways. *In vivo* experiments further demonstrated that GSG2 knockdown suppressed tumor growth. In summary, GSG2 was involved in the progression of CCA, suggesting that GSG2 may be a potential therapeutic target for CCA patients.

Correspondence to: Dr Ranglang Huang, Department of Hepatobiliary and Pancreatic Surgery, The Third Xiangya Hospital of The Central South University, 138 Tongzhipo Road, Yuelu, Changsha, Hunan 410013, P.R. China
E-mail: huangranglang@csu.edu.cn

Key words: cholangiocarcinoma, GSG2, proliferation, apoptosis, cell cycle, migration

Introduction

Cholangiocarcinoma (CCA) originates from the epithelium lining of the biliary tree and is classified into intrahepatic cholangiocarcinoma (iCCA) and extrahepatic cholangiocarcinoma (eCCA), which is further stratified into perihilar (pCCA) and distal (dCCA) cholangiocarcinoma (1,2).Cholangiocarcinoma is the second most common primary hepatobiliary malignancy after hepatocellular carcinoma (HCC) (3,4). Most patients with CCA are diagnosed in the advanced and metastatic stages of the disease due to lack of signs and symptoms in the early stage (3). Unfortunately, CCA is an invasive malignancy with a median survival of less than 2 years from diagnosis (5). This fact, as well as the adverse outcomes of the current use of local and systemic therapy, is the cause of poor prognosis in CCA patients and strongly supports the need for new therapeutic drugs and strategies (6). The molecular mechanisms of CCA have been partially identified in recent years, including isocitrate dehydrogenase (*IDH1* and *IDH2*) mutations and fibroblast growth factor receptor 2 (FGFR2) fusions, as well as gene mutations involved in chromatin remodeling, such as AT-rich interaction domain 1A (*ARID1A*), protein poly-bromo 1 (*PBRM1*), and BRCA1-associated protein 1 (*BAP1*) (7,8). Elucidation of key molecules involved in CCA development, inhibition of certain mutated genes or inhibition of related signaling pathways through specific inhibitors opens new horizons for novel therapeutic approaches (9,10). Thus, a deeper understanding of CCA molecular mechanisms is needed to lay the foundation for targeted therapy.

Germ cell-specific gene 2 protein (GSG2), also termed histone H3 phosphorylated by GSG2 at threonine-3, is mainly expressed in haploid germ cells (11,12). GSG2 has been shown to be weakly expressed in proliferating normal somatic cells but plays a crucial role in mitosis, where it specifically phosphorylates Thr-3 in histone H3 (H3T3) (12-14). On the other hand, GSG2 does not belong to the family of eukaryotic protein kinase, which is a structurally unique kinase and may result in fewer off-target effects (15). GSG2 RNAi in tumor cells prevents chromosome alignment and normal mitosis, suggesting that GSG2 inhibitors may be a novel anti-mitotic agent that prevents cancer cell proliferation (16,17). For instance, GSG2 knockdown was found to inhibit progression and development of pancreatic cancer *in vitro* and *in vivo* (18).

Recently, Yu *et al* found that GSG2 knockdown inhibited cell proliferation, colony formation and induced apoptosis, and may serve as a potential therapeutic target for prostate cancer therapy (19). Ample evidence suggests that identifying specific GSG2 inhibitors may be feasible and useful for basic biological studies and as candidates for cancer therapy (20-23). Therefore, we were committed to exploring the molecular mechanisms of GSG2 in CCA to determine whether GSG2 inhibitors have the potential to be molecular anticancer drugs against CCA.

In the present study, the role and mechanisms of GSG2 in the regulation of CCA progression and development were explored. First, we found that GSG2 was abundantly expressed in CCA and its expression was positively correlated with pathological grade. Additionally, it was revealed that GSG2 knockdown inhibited cell proliferation, migration, promoted cell apoptosis and arrested the cell cycle in the G2 phase. These findings highlight the significance of GSG2 in CCA and confirm its therapeutic potential.

Materials and methods

Tissue microarray chip. A total of 80 cases/80 points of microarray chips of CCA were purchased from Xi'an Alina Biotechnology Co., Ltd. (Xi'an, China). These included 75 cases of tumor tissues (48 cases of eCCA, 27 cases of iCCA) and 5 cases of para-carcinoma tissues (intrahepatic bile duct tissue). These paraffin-embedded human tissue chips were 1.5 mm in diameter and 5 μm in thickness and stored immediately at -4˚C for later use. The study was approved by the Ethics Committee of The IRB of The Third Xiangya Hospital, Central South University (no. 2019-S435).

Cell culture. The human CCA cell lines HCCC-9810, QBC939 and HuCCT1 were obtained from the Cell Bank of the Chinese Academy of Sciences (Shanghai, China). Human intrahepatic bile duct epithelial cells (HIBECs) were purchased from Beina Biotechnology Research Institute (http://www.bnbio.com/pro/p1/1/p_3391.html, Beijing, China). These cells were cultured in RPMI-1640 medium (Gibco; Thermo Fisher Scientific, Inc.) together with 10% fetal bovine serum (FBS), 100 mg/ml streptomycin plus, and 100 IU/ml of penicillin (Gibco; Thermo Fisher Scientific, Inc.) in an atmosphere of 5% CO_2 at 37˚C.

Immunohistochemical (IHC) staining. The tissue microarray chips were stained with DAB solution and then with hematoxylin. In brief, the tissue microarray chip was immersed in xylene and ethanol in turn dewaxed and rehydrated. The chip was boiled in 10 mM sodium citrate buffer (pH 6. 0) and maintained for 10 min. After that, the chip was cooled and soaked in distilled water for cleaning. To permeabilize the tissue, the chip was washed twice with 1% animal serum in PBS with 0.4% Triton X-100 (PBS-T). The primary antibody GSG2 (dilution 1:200, Bioss, cat. # bs-15413R) was diluted in 1% animal serum in PBS-T and incubated at room temperature for 2 h. The incubation was continued overnight at 4˚C in a humidified chamber. Subsequently, the secondary antibody goat anti-rabbit (dilution 1:200, Beyotime Institute of Biotechnology, cat. # A0208) was immersed for 2 h at room temperature. Subsequently, the chips were stained with DAB solution as well as hematoxylin, and photographed with a microscope (magnification, x200 and x400) (MicroPublisher 3.3RTV; Olympus, Tokyo, Japan), and viewed with ImageScope (ScanScope XT) and CaseViewer. IHC total scores were determined by staining percentage scores [classified as: 1 (1-24%), 2 (25-49%), 3 (50-74%), 4 (75-100%)] and staining intensity scores (scored as 0, slight color; 1, brown; 2, light yellow; 3, dark brown). Finally, high or low expression of GSG2 was determined by the median of the IHC experimental scores of all tissues.

Cell transfection, lentivirus production and infection. For knockdown of GSG2, small interfering RNAs specifically targeting GSG2 (shGSG2-1, shGSG2-2, shGSG2-3) (Table SI) were designed by Shanghai YiBeiRui Biomedical Science and Technology Co., Ltd. and negative controls were scramble siRNAs (shCtrl) (sequences are detailed in Table SI). The shGSG2 sequences were inserted into BR-V108 vectors (Shanghai YiBeiRui, China) containing green fluorescent protein (GFP) which acted as a detectable marker.

HCCC-9810, QBC939 and HuCCT1 cells were seeded into 6-well plates (Corning Inc.) at an approximate density of $2x10^5$ cells per well. Subsequent to a 24-h cultivation, the cells were infected with 100 μl lentiviral vectors ($1x10^7$ TU/ml) added to ENI.S and polybrene (10 μg/ml, Sigma-Aldrich; Merck KGaA). Next, the reconstructed vectors were introduced into 293T cells for the generation of lentiviruses, together with pHelper 1.0 and pHelper 2.0 (Shanghai YiBeiRui Biomedical Science and Technology) as packing vectors. Following infection for 72 h, the supernatants containing the lentivirus expressing shGSG2 or shCtrl were harvested. Subsequently, qPCR analysis and western blot analysis were used to evaluate the GSG2 knockdown efficiency. Finally, the successfully infected cells were subjected to the following function assays.

qPCR. HCCC-9810 and QBC939 cell RNA was isolated with Trizol reagent (Invitrogen; Thermo Fisher Scientific, Inc.) with DNase I (Vazyme) according to the manufacturer using a standard procedure. RNA was converted into cDNA using the M-MLV RT kit (Promega Corp.). cDNA was amplified with SYBR Green Master Mix kit (Vazyme) and Bio-Rad CFX96 sequence detection system (Bio-Rad Laboratories, Inc.). Sequences are detailed in Table SII and GAPDH was used as an internal reference. Results of qPCR were evaluated using the $2^{-\Delta\Delta Cq}$ method (24) and converted into fold change.

Western blotting (WB). HCCC-9810 and QBC939 cells were fully lysed in ice-cold RIPA buffer (Millipore) to obtain protein. The protein concentration detection was performed using the HyClone-Pierce™ BCA Protein Assay kit (Thermo Fisher Scientific, Inc., cat. # 23225). Protein (20 μg) per group was separated by 10% SDS-PAGE, transferred onto PVDF membranes, and analyzed with required primary antibodies and the corresponding secondary antibodies in turn (antibodies are detailed in Table SIII) at room temperature for 2 h. The blots were visualized by Amersham ECL plus TM Western Blot system (GE Healthcare Life Sciences) and the density of the protein band was analyzed by ImageJ (National Institutes of Health, v1.8.0).

Table I. Expression patterns in cholangiocarcinoma cancer tissues and para-carcinoma tissues revealed by immunohistochemistry analysis.

GSG2 expression	Tumor tissue		Para-carcinoma tissue		P-value
	Cases	Percentage	Cases	Percentage	
Low	37	49.3%	5	100%	<0.001
High	38	50.7%	0	-	

GSG2, germ cell-specific gene 2 protein.

Table II. Relationship between GSG2 expression and tumor characteristics in patients with cholangiocarcinoma cancer.

Features	No. of patients	GSG2 expression		P-value
		Low	High	
All patients	75	37	38	
Age (years)				0.7301456
<59	37	19	18	
≥59	38	18	20	
Sex				0.7253323
Male	39	20	19	
Female	36	17	19	
Tumor grade				1.1793e-06
1	10	9	1	
2	38	23	15	
3	23	2	21	
Lymphatic metastasis (N)				0.06172829
N0	58	32	26	
N1	17	5	12	
T infiltrate				0.1400056
T1	6	5	1	
T2	34	13	21	
T3	32	18	14	
T4	3	1	2	

GSG2, germ cell-specific gene 2 protein.

MTT assay. Following trypsinization of the HCCC-9810 and QBC939 cells in each experimental group while in the logarithmic growth phase, cells (2,000 cells/well) were seeded onto a 96-well plate overnight. A total of 20 μl of a 5 mg/ml MTT solution (Genview, cat. # JT343) was added to each well 4 h prior to termination of the culture. After incubation for 4 h, 100 μl dimethyl sulfoxide (DMSO) was added to each well. Following that, formazan was quantified at 24, 48, 72, 96 and 120 h by measuring the absorbance at 490 nm with a microplate reader. The absorbance was associated with the percentage of viable cells, and the cell viability ratio was calculated according to the following formula: Cell viability (%) = optical density (OD) treated/OD control x100%.

Table III. Correlation between GSG2 expression and tumor characteristics in patients with cholangiocarcinoma cancer.

		GSG2
Grade	Pearson related	0.575
	Significance (double tail)	<0.001
	N	71

GSG2, germ cell-specific gene 2 protein.

Cell cycle analysis by flow cytometry. HCCC-9810 and QBC939 cells were inoculated in 6-well plates (Corning Inc.) until cell density reached 85%. Afterwards, these cells were harvested, centrifuged (1,200 x g), and resuspended. The cells were fixed with pre-cooled 70% ethanol (4˚C) for at least 1 h, the ethanol was removed, and the cells were washed once with PBS. Subsequently, the cells were stained with 1 ml cell staining solution [40X PI (BD Biosciences), 2 mg/ml: 100X RNase, 10 mg/ml: 1X PBS = 25:10:1,000) for 30 min. Fluorescence activated cell analysis (FACS)/FACScan and FlowJo 7.6.1 (FlowJo, LLC)/CellQuest Pro software (BD Biosciences) were used for analysis. The percentage of the cells in the G0-G1, S, and G2-M phases were counted and compared.

Cell apoptosis analysis by flow cytometry. After HCCC-9810 and QBC939 cells were inoculated in 6-well plates at a seeding density of $1x10^3$ cells/ml for 10 day, washed with PBS and harvested by centrifugation at 3,000 x g for 10 min, the supernatant was discarded. The cells were washed once again with PBS, centrifuged, and the supernatant was discarded, and the cells were resuspended by adding 500 μl of diluted 1X Annexin V Binding Buffer working solution. Annexin V-APC (10 μl) was added for staining for 10-15 min at room temperature without light. The percentage of cells in the different phases was measured using FACSCanto II Flow Cytometry (BD Bioscience) to assess the apoptotic rate, and the results were analyzed.

Human apoptosis antibody array. For signal pathway gene detection, the Human Apoptosis Antibody Array (Abcam, cat. # ab134001) was applied following the manufacturer's instructions. Briefly, QBC939 cells were lysed in cold RIPA buffer (Millipore), and the protein concentration was detected by BCA Protein Assay kit (HyClone-Pierce; Thermo Fisher Scientific, Inc.). Proteins were incubated with a blocked array antibody membrane overnight at 4˚C. After washing, Detection Antibody Cocktail (1:100) was added and incubation was carried out for 1 h, followed by incubated with HRP linked streptavidin conjugate for 1 h. All spots were visualized by enhanced ECL and the signal densities were analyzed with Image J software (National Institute of Health, v1.8.0).

Wound-healing assay. HCCC-9810 and QBC939 cells were cultivated into 6-well plates and were grown until reaching 90% confluence. On the following day, a 10-μl pipette was used to scratch a wound at the middle of each well. Then,

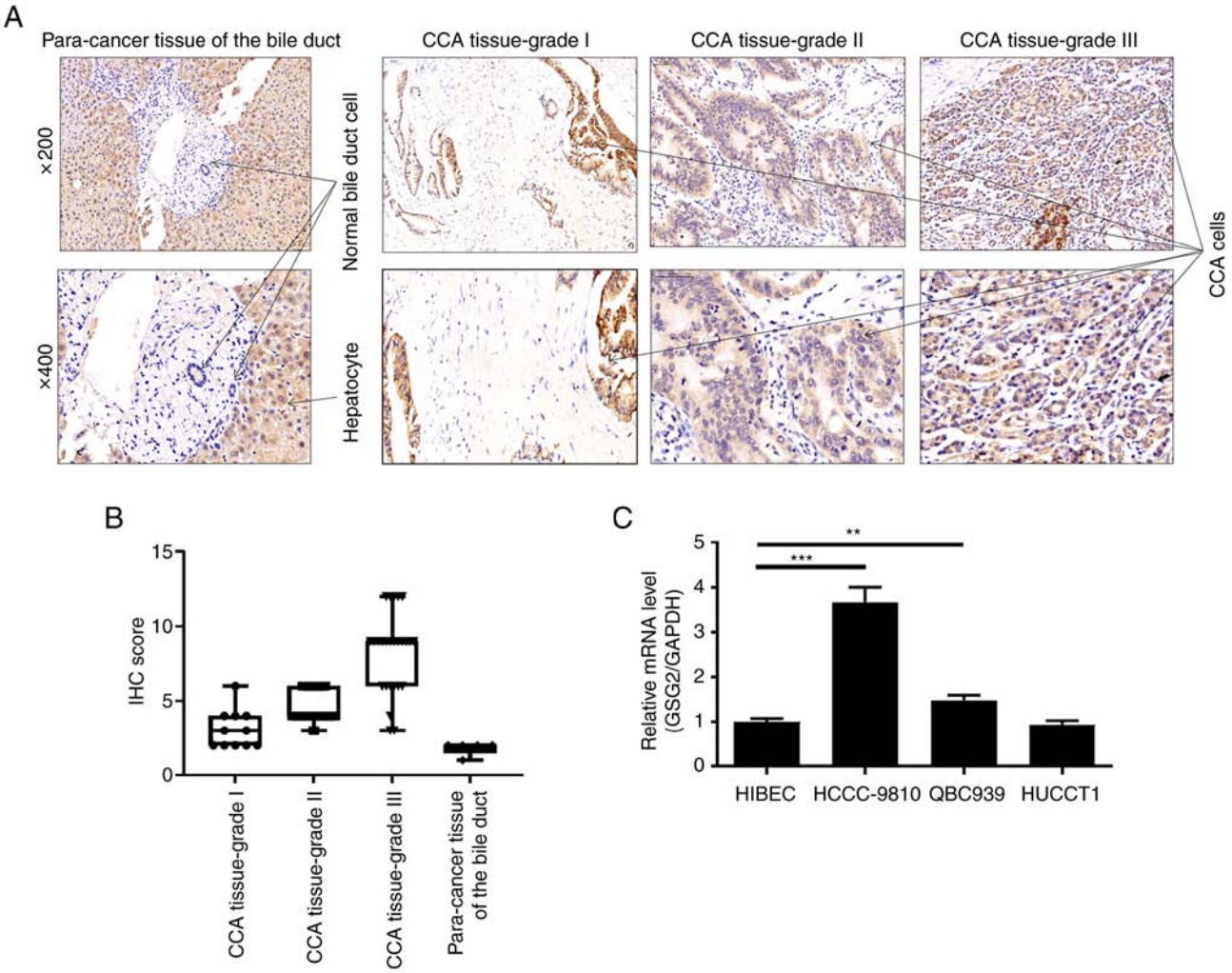

Figure 1. GSG2 is highly expressed in CCA. (A) Expression levels of GSG2 in CCA tumor tissues and adjacent normal skin tissues were detected by IHC staining. (B) The IHC scores of GSG2 in CCA tumor tissues of different grades and para-cancer tissue of the bile duct are presented. (C) GSG2 expression in human CCA cell lines HCCC-9810, QBC939 and HuCCT1 and human intrahepatic bile duct epithelial cells (HIBECs) was detected by qPCR. Data are presented as the mean ± SD (n=3). **P<0.01, ***P<0.001. GSG2, germ cell-specific gene 2 protein; CCA, cholangiocarcinoma.

the medium was substituted with 1% FBS-containing fresh medium. Images of the wounds were captured at pre-set time points (4, 8, 24 and 48 h). The cell migration rate of each group was calculated based on the images and analyzed using NIH ImageJ software.

Animal xenograft model. Animal experiments were approved by the Ethics Committee of The IRB of The Third Xiangya Hospital, Central South University and conducted in accordance with guidelines and protocols for animal care and protection. The four-week-old male BALB/c nude mice (15±0.73 g) (Shanghai Lingchang Biotechnology Co., Ltd) were housed under pathogen-free condition at room temperature for the xenograft model. Twenty mice were injected with $4x10^6$ HuCCT1 cells and randomly divided into two groups, shCtrl and shGSG2. Mice weight and tumor volume were detected twice a week after 10 days of subcutaneous injection. Tumor volume = π/6 x L x W x W, where L is the long diameter and W is the short diameter. On the 32th day after cell injection, 0.7% pentobarbital sodium at a dose of 40 mg/kg was injected into the abdominal cavity to anesthetize the mice (25-27), and the bioluminescence imaging intensity (IVIS spectral imaging system, emission wavelength of 510 nm) was observed. After 32 days of subcutaneous injection, the experimental animals were sacrificed by cervical dislocation ensuring that the mice died instantly and without suffering. The tumors were removed and weighed.

Ki67 staining. Mouse tumor tissues were fixed in 10% formalin and then were paraffin-embedded. Sections (5-μm) were cut and immersed in xylene and ethanol. Tissue slides were blocked with 3% PBS-H_2O_2 and incubated with anti-Ki67 (dilution 1:200, Abcam, cat. # ab16667) and HRP goat anti-rabbit IgG (dilution 1:400, Abcam, cat. # ab6721). Subsequently, the slides were stained with DAB solution as well as hematoxylin, and examined at x100 and x200 with an objective lens microscope.

Statistical analysis. All experiments were conducted in triplicate, and data are shown as mean ± SD. Statistical analyses and graphical representations were carried out by GraphPad Prism 7.0 (Graphpad Software, Inc.) and a P-value <0.05 was indicative of a statistically significant difference. The significance difference between groups was determined using

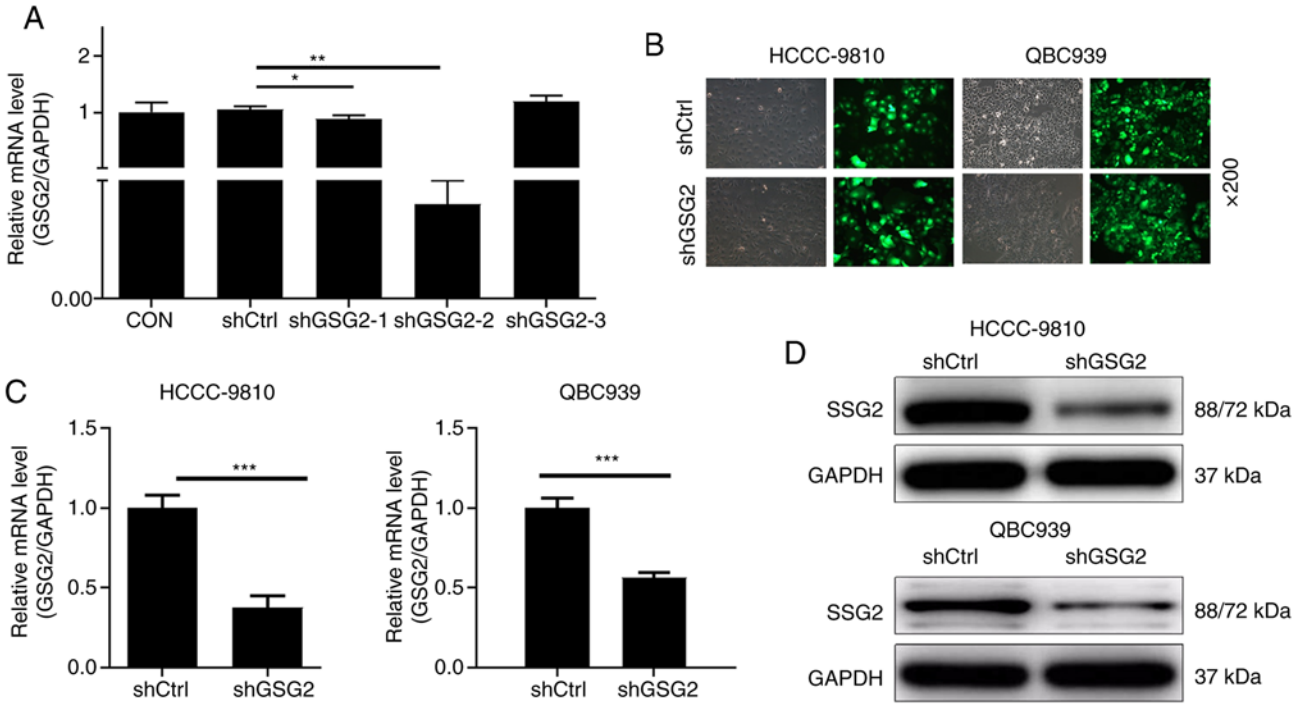

Figure 2. Construction of the GSG2 knockdown cell model. (A) qPCR was used to screen knockdown efficiency of GSG2 in the shGSG2-1, shGSG2-2, and shGSG2-3 groups. (B) Transfection efficiencies in CCA HCCC-9810 and QBC939 cells were evaluated by expression of green fluorescent protein 72 h post-infection. (C and D) The specificity and validity of the lentivirus-mediated shRNA knockdown of GSG2 expression was verified by qPCR (C) and WB analysis (D). Data are presented as the mean ± SD (n=3). *P<0.05, **P<0.01, ***P<0.001. GSG2, germ cell-specific gene 2 protein; CCA, cholangiocarcinoma; WB, western blotting; CON, control.

the two-tailed Student's t-test or one-way ANOVA followed by Bonferroni's post hoc test analysis. GSG2 expression in tumor tissues and normal tissues revealed in the IHC assay were analyzed with Sign test. Relationship between GSG2 expression and tumor characteristics in patients with CCA was analyzed using the Chi-square test or Fisher's exact test.

Results

High expression of GSG2 in CCA. According to the results of the IHC staining, expression of GSG2 in CCA tissues was significantly higher than that in normal tissues (P<0.001) (Table I, Fig. 1A). Subsequently, the results of the Chi-square test or Fisher's exact test revealed a significant correlation between GSG2 expression and pathological tumor grade (Table II, Fig. 1B). Notably, the pathological grade of cholangiocarcinoma was classified according to the protocol provided in the literature (28). Consistently, Spearman grade correlation analysis further confirmed that GSG2 expression was positively correlated with pathological grade (Table III). More specifically, the increase in GSG2 expression was accompanied by CCA deterioration. Besides, we also found that mRNA levels of GSG2 were significantly highly expressed in CCA cell lines HCCC-9810 and QBC939 when compared to the HIBEC cell line (Fig. 1C). Taken together, high expression of GSG2 in CCA has significant clinical significance in predicting disease deterioration.

Construction of the GSG2-knockdown CCA cell model. Firstly, qPCR analysis determined that the transfection efficiency of GSG2 in the shGSG2-2 group was 99.6% and it was used in the following experiments (P<0.01) (Fig. 2A). Furthermore, the percentage of GFP-positive cells infected with shCtrl or shGSG2 for 72 h observed under fluorescence microscope was more than 80% (Fig. 2B). The results of qPCR showed that in the HCCC-9810 and QBC939 cells, compared with the relevant shCtrl group, the knockdown efficiency of GSG2 in the shGSG2 group was 62.4% (P<0.001) and 43.6% (P<0.001), respectively (Fig. 2C). Not surprisingly, the results of the WB analysis showed a consistent downregulation of protein expression in HCCC-9810 and QBC939 cells compared with the controls (Fig. 2D). The above results clearly revealed that the CCA cell model of GSG2 knockdown was successfully constructed.

Knockdown of GSG2 inhibits CCA cell proliferation in vitro. The results of the MTT assays are presented as (P<0.001) Fig. 3A. Cell proliferation of the HCCC-9810 and QBC939 cells in the shGSG2 group was obviously slower compared with the shCtrl group. These results indicated that viable cells were both reduced as time goes on after knockdown of GSG2. All in all, GSG2 knockdown has a certain inhibitory effect on CCA cell proliferation.

Knockdown of GSG2 arrests cell cycle and promotes CCA cell apoptosis in vitro. Cell cycle and cell apoptosis were assessed using flow cytometry. The results of the cell cycle distribution detection showed that the percentages of cells in the S phase were significantly decreased whereas the percentages of cells in the G2 phase were significantly increased in the shGSG2 group, compared with the shCtrl groups (P<0.001) (Fig. 3B). Moreover, the ratio of apoptotic

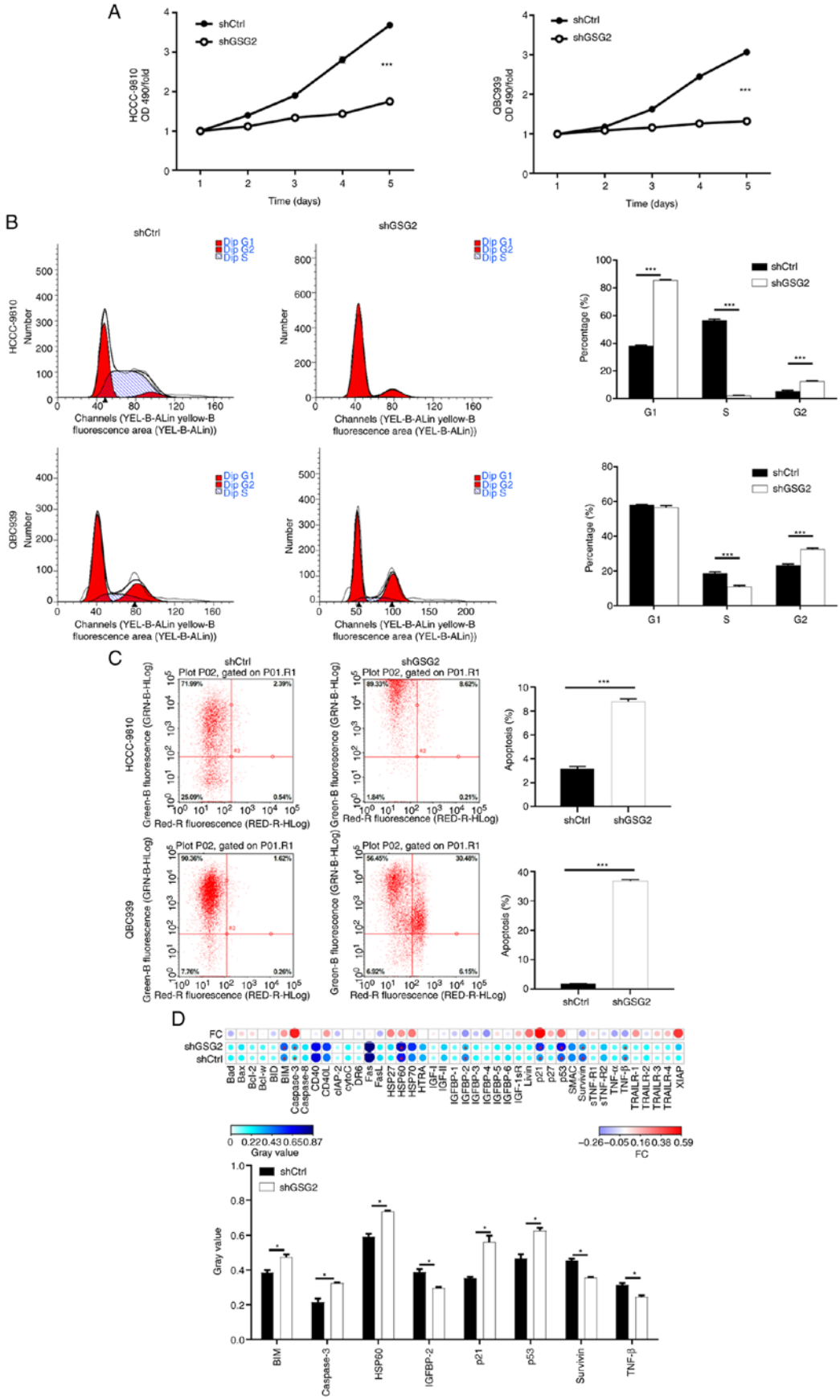

Figure 3. Knockdown of GSG2 inhibits cell proliferation, arrests cell cycle at G2 and promotes apoptosis in CCA cells. (A) Cell proliferation of CCA HCCC-9810 and QBC939 cells with or without knockdown of GSG2 was evaluated by MTT assay. ***P<0.001, shGSG2 vs. shCtrl group. (B and C) Flow cytometric analysis based on Annexin V-APC staining was utilized to detect cell cycle distribution (B) and cell apoptotic ratio (C) in the HCCC-9810 and QBC939 cells. (D) Human apoptosis antibody array analysis was performed using QBC939 cells with or without GSG2 knockdown. Data are presented as mean ± SD (n=3), *P<0.05, ***P<0.001. GSG2, germ cell-specific gene 2 protein; CCA, cholangiocarcinoma; BIM, Bcl-2-like protein 11; HSP60, heat shock protein 60; IGFBP-2, insulin-like growth factor-binding protein 2; TNF-β, tumor necrosis factor-β.

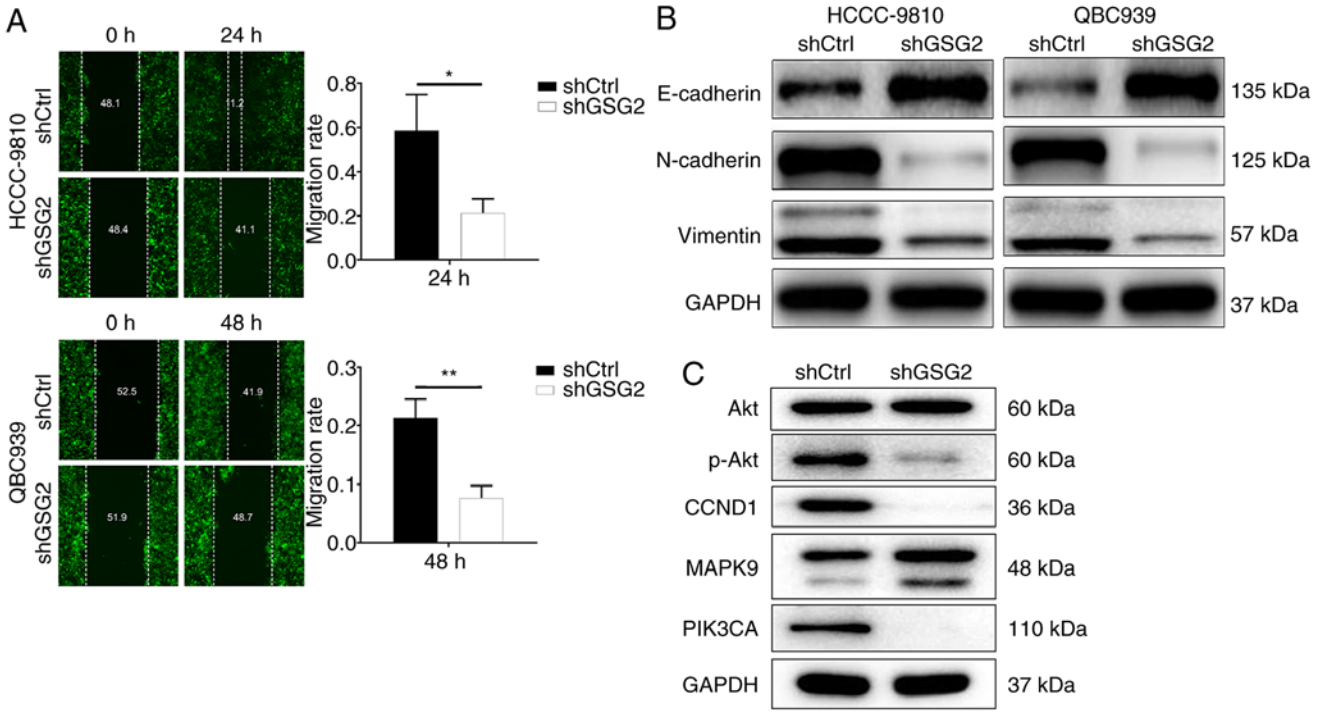

Figure 4. Effects of GSG2 knockdown on CCA cell migration and downstream molecular mechanisms. (A) Cell migration of CAA HCCC-9810 and QBC939 cells with or without knockdown of GSG2 was evaluated by wound healing assay. (B) EMT marker proteins of HCCC-9810 and QBC939 cells with or without knockdown of GSG2 were detected by WB. (C) The expression of the downstream protein pathway was observed by WB in QBC939 cells with or without GSG2 knockdown. Data are presented as mean ± SD (n=3), *P<0.05, **P<0.01. GSG2, germ cell-specific gene 2 protein; CCA, cholangiocarcinoma; EMT, epithelial-to-mesenchymal transition; WB, western blotting; CCND1, cyclin D1; PIK3CA, phosphatidylinositol-4,5-bisphosphate 3-kinase; MAPK9, mitogen-activated protein kinase 9.

cells in the shGSG2 groups of HCCC-9810 and QBC939 cells was significantly higher than that in the shCtrl groups (P<0.001) (Fig. 3C). Thus, the comprehensive results suggest that GSG2 knockdown arrests the cell cycle in the G2 phase and promotes the apoptosis of CCA cells. The expression of related proteins in the human apoptosis signaling pathway was detected after the knockdown of GSG2 in QBC939 cells, showing that the protein expression levels of Bcl-2-like protein 11, commonly called BIM, caspase3, heat shock protein 60 (HSP60), p21, p53 were significantly upregulated, while the protein expression of insulin-like growth factor-binding protein 2 (IGFBP-2), survivin and tumor necrosis factor (TNF)-β was obviously downregulated (P<0.05) (Fig. 3D).

Knockdown of GSG2 inhibits CCA cell migration in vitro. The migration capacity of CCA cells with or without GSG2 knockdown was identified by wound-healing assay. The results displayed that the migration rate of HCCC-9810 cells in the shGSG2 group at 24 h was decreased by 57% compared with the shCtrl group (P<0.001). Meanwhile, the migration rate of QBC939 cells at 48 h was decreased by 83% (P<0.001) (Fig. 4A). Additionally, the expression of EMT biomarkers was detected by WB, indicating that the protein level of E-cadherin was upregulated in the shGSG2 group compared with the shCtrl group in the HCCC-9810 and QBC939 cells; contrarily, protein expression of N-cadherin and vimentin were downregulated (Fig. 4B). Obviously, knockdown of GSG2 inhibited CCA cell migration by suppressing N-cadherin and vimentin.

Exploration of downstream molecular mechanism of GSG2 in CCA. The downstream molecular mechanism of GSG2 in CCA cell was elicited through WB (Fig. 4C). The results showed that the protein expression of phosphorylated (p-)Akt, cyclin D1 (CCND1) and phosphatidylinositol-4,5-bisphosphate 3-kinase (PIK3CA) was downregulated in the experimental group compared with the control group; while mitogen-activated protein kinase 9 (MAPK9) protein expression was upregulated, and there was no significant alteration in Akt. In brief, GSG2 is involved in the progression of CCA by regulating apoptosis-related factors and downstream signaling.

Knockdown of GSG2 in CCA cells impairs tumor growth in vivo. HuCCT1 cells infected with shGSG2 or shCtrl were subcutaneously injected into nude mice to establish the xenograft model, and the GSG2 expression of shGSG2 and shCtrl in mouse tumor tissue was detected by WB (Fig. S1). The results showed that the expression of GSG2 in the shGSG2 tumor group was significantly lower than that in the shCtrl group, which confirmed the inhibition efficiency of GSG2 in the targeted xenografts derived from the injected HuCCT1 cells.

Importantly, the average tumor volume in the shGSG2 group was significantly reduced by 33.85±10.92 mm^3 compared with the shCtrl group (P<0.01) (Fig. 5A). In particular, the average tumor weight of mice inoculated with shGSG2 cells was significantly lower than that of the shCtrl group (P<0.01) (Fig. 5B). Additionally, *in vivo* imaging indicated that bioluminescence expression was apparently weaker in the shGSG2 group than that in the shCtrl group (P<0.01), also indicating the

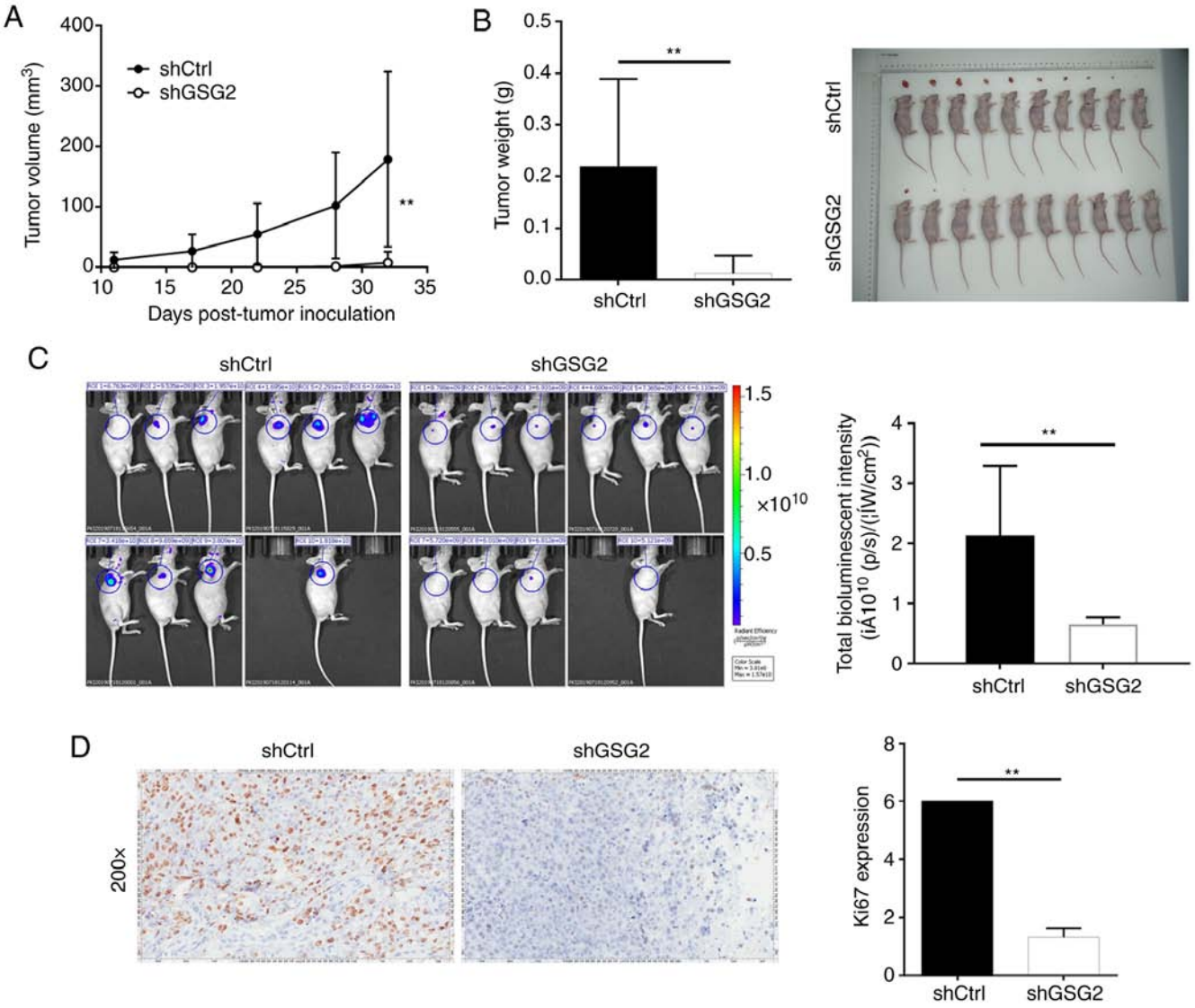

Figure 5. Knockdown of GSG2 inhibits tumor growth in mouse xenograft models. (A) The volume of tumors in the shCtrl group and shGSG2 group was measured after post-injection. (B) The images and average weight of tumors in the shCtrl group and shGSG2 group. (C) The imaging and total bioluminescent intensity of tumors in the shCtrl group and shGSG2 group. (D) The staining images and expression levels of Ki67 in tumor tissues in the shCtrl group and shGSG2 group. Data are presented as mean ± SD (n=3), **P<0.01. GSG2, germ cell-specific gene 2 protein.

lower tumor burden in the shGSG2 group (Fig. 5C). Moreover, Ki67 staining displayed that the proliferative activity of tumors in the shGSG2 group was significantly lower than that in the shCtrl group (P<0.01) (Fig. 5D). In a word, knockdown of GSG2 impaired tumorigenicity *in vivo*, which was in accordance with the aforementioned *in vitro* results.

Discussion

The physiological function of germ cell-specific gene 2 protein (GSG2) has not been well illustrated, and the underlying mechanism associated with tumor progression is far from clear. In the present study, it was demonstrated that GSG2 promoted the development of cholangiocarcinoma (CCA). Through loss-of-function experiments, it was demonstrated that GSG2 knockdown significantly suppressed cell proliferation, migration and tumor growth. Conversely, CCA cell apoptosis was obviously promoted upon GSG2 knockdown, which may have resulted from the regulation of apoptosis-related proteins such as BIM, caspase3, HSP60, p21, p53, IGFBP-2, survivin and TNF-β.

Unlimited growth, aggressiveness, reduced apoptosis and cell cycle disorders are markers of cancer and play an important role in the development of cancer (29). Moreover, apoptosis is a key biological process by which to prevent uncontrolled cell proliferation and eliminate harmful cells, and anti-apoptotic stimulation is a hallmark of various types of cancer (30,31). Mechanisms of apoptosis and their effector proteins include pro-apoptotic protein, anti-apoptotic Bcl-2 family members, and inhibitor of apoptosis proteins (IAP) (31). BIM, caspase3, HSP60, p21 and p53 are all pro-apoptotic proteins, which may contribute to apoptosis induction (32-35). Caspase3 functions as an executor of apoptosis by activating DNA fragmentation (36). Alternatively, IGFBP-2 plays an important role in cell proliferation, invasion, angiogenesis and apoptosis (37). Simultaneously, survivin, as an important member of the IAP family, is considered to be a regulator of apoptosis-related proteins and prevents apoptosis, and it was strongly expressed

in CCA (38-40). TNF-β also was identified as a key mediator between apoptosis and cancer cell progression (41). Thus, it was possible that GSG2 knockdown initiated the process of apoptosis through balancing the expression of pro-apoptotic and anti-apoptotic factors.

We further revealed that GSG2 may regulate cell migration by influencing EMT-related proteins. Research has confirmed that epithelial-to-mesenchymal transition (EMT) promotes invasion and metastasis in various types of tumors (42). This process involves the downregulation of epithelial-specific marker E-cadherin and upregulation of mesenchymal markers including vimentin, and N-cadherin (43). In our study, knockdown of GSG2 inhibited CCA cell migration by inducing EMT, which included E-cadherin upregulation and N-cadherin and vimentin downregulation.

Moreover, we estimated that GSG2 was involved in CCA progression via Akt signaling. Previous studies have revealed that PI3K/Akt, CCND1/CDK6 and MAPK pathways play a key role in the development of CCA (44-47). For example, Wang *et al* clarified that TSPAN1 is involved in CCA progression via the PI3K/Akt pathway (47). Zhang *et al* suggested that S100A11 promotes cell proliferation by the p38/MAPK signaling pathway in iCCA (48). This study discovered that GSG2 knockdown contributed to downregulation of P-Akt, CCND1, PIK3CA, and upregulation of MAPK9. Therefore, we suggest that GSG2 exerts effects on CCA cells by modulating protein pathways, such as PI3K/Akt, CCND1/CDK6 and MAPK9.

The present study found that expression of GSG2 was positively associated with pathological grade. Importantly, we revealed that GSG2 knockdown inhibited CCA cell progression by regulating cell proliferation, apoptosis, cell cycle distribution, and cell migration. In summary, the role and preliminary regulatory mechanisms of GSG2 in CCA were demonstrated, suggesting that GSG2 may be a potential therapeutic target for CCA patients.

Acknowledgements

Not applicable.

Funding

No funding was received.

Availability of data and materials

According to reasonable request, the datasets used in this study are available from the corresponding author.

Authors' contributions

RH designed the research study. JZ, JY and CW conducted the cell experiments. WN performed the animal experiments. ZZ and LM carried out the data collection and analysis. JZ produced the manuscript which was checked and revised by RH. All authors read and approved the manuscript and agree to be accountable for all aspects of the research in ensuring that the accuracy or integrity of any part of the work are appropriately investigated and resolved.

Ethics approval and consent to participate

Animal experiments were approved by the Ethics Committee of The IRB of The Third Xiangya Hospital, The Central South University and conducted in accordance with guidelines and protocols for animal care and protection.

Patient consent for publication

Not applicable.

Competing interests

The authors declare that they have no competing interests.

References

1. Lowery MA, Ptashkin R, Jordan E, Berger MF, Zehir A, Capanu M, Kemeny NE, O'Reilly EM, El-Dika I, Jarnagin WR, *et al*: Comprehensive molecular profiling of intrahepatic and extrahepatic cholangiocarcinomas: Potential targets for intervention. Clin Cancer Res 24: 4154-4161, 2018.
2. Esnaola NF, Meyer JE, Karachristos A, Maranki JL, Camp ER and Denlinger CS: Evaluation and management of intrahepatic and extrahepatic cholangiocarcinoma. Cancer 122: 1349-1369, 2016.
3. Patel N and Benipal B: Incidence of cholangiocarcinoma in the USA from 2001 to 2015: A US Cancer Statistics Analysis of 50 States. Cureus 11: e3962, 2019.
4. Goldaracena N, Gorgen A and Sapisochin G: Current status of liver transplantation for cholangiocarcinoma. Liver Transpl 24: 294-303, 2018.
5. Ustundag Y and Bayraktar Y: Cholangiocarcinoma: A compact review of the literature. World J Gastroenterol 14: 6458-6466, 2008.
6. Blechacz B: Cholangiocarcinoma: Current knowledge and new developments. Gut Liver 11: 13-26, 2017.
7. Fouassier L, Marzioni M, Afonso MB, Dooley S, Gaston K, Giannelli G, Rodrigues CMP, Lozano E, Mancarella S, Segatto O, *et al*: Signalling networks in cholangiocarcinoma: Molecular pathogenesis, targeted therapies and drug resistance. Liver Int 39 (Suppl 1): S43-S62, 2019.
8. Simile MM, Bagella P, Vidili G, Spanu A, Manetti R, Seddaiu MA, Babudieri S, Madeddu G, Serra PA, Altana M and Paliogiannis P: Targeted therapies in cholangiocarcinoma: Emerging evidence from clinical trials. Medicina (Kaunas) 55: 42, 2019.
9. Rizvi S, Khan SA, Hallemeier CL, Kelley RK and Gores GJ: Cholangiocarcinoma-evolving concepts and therapeutic strategies. Nat Rev Clin Oncol 15: 95-111, 2018.
10. Labib PL, Goodchild G and Pereira SP: Molecular pathogenesis of cholangiocarcinoma. BMC Cancer 19: 185, 2019.
11. Sato S, Maeda C, Hattori N, Yagi S, Tanaka S and Shiota K: DNA methylation-dependent modulator of Gsg2/Haspin gene expression. J Reprod Dev 57: 526-533, 2011.
12. Tanaka H, Yoshimura Y, Nozaki M, Yomogida K, Tsuchida J, Tosaka Y, Habu T, Nakanishi T, Okada M, Nojima H and Nishimune Y: Identification and characterization of a haploid germ cell-specific nuclear protein kinase (Haspin) in spermatid nuclei and its effects on somatic cells. J Biol Chem 274: 17049-17057, 1999.
13. Higgins JM: The Haspin gene: Location in an intron of the integrin alphaE gene, associated transcription of an integrin alphaE-derived RNA and expression in diploid as well as haploid cells. Gene 267: 55-69, 2001.
14. Eswaran J, Patnaik D, Filippakopoulos P, Wang F, Stein RL, Murray JW, Higgins JM and Knapp S: Structure and functional characterization of the atypical human kinase haspin. Proc Natl Acad Sci USA 106: 20198-20203, 2009.
15. Higgins JM: Haspin-like proteins: A new family of evolutionarily conserved putative eukaryotic protein kinases. Protein Sci 10: 1677-1684, 2001.
16. Dai J, Sultan S, Taylor SS and Higgins JM: The kinase haspin is required for mitotic histone H3 Thr 3 phosphorylation and normal metaphase chromosome alignment. Genes Dev 19: 472-488, 2005.

17. Patnaik D, Jun X, Glicksman MA, Cuny GD, Stein RL and Higgins JM: Identification of small molecule inhibitors of the mitotic kinase haspin by high-throughput screening using a homogeneous time-resolved fluorescence resonance energy transfer assay. J Biomol Screen 13: 1025-1034, 2008.
18. Han X, Kuang T, Ren Y, Lu Z, Liao Q and Chen W: Haspin knockdown can inhibit progression and development of pancreatic cancer in vitro and vivo. Exp Cell Res 385: 111605, 2019.
19. Yu F, Lin Y, Xu X, Liu W, Tang D, Zhou X, Wang G, Zheng Y and Xie A: Knockdown of GSG2 inhibits prostate cancer progression *in vitro* and *in vivo*. Int J Oncol 57: 139-150, 2020.
20. Yi Q, Chen Q, Yan H, Zhang M, Liang C, Xiang X, Pan X and Wang F: Aurora B kinase activity-dependent and -independent functions of the chromosomal passenger complex in regulating sister chromatid cohesion. J Biol Chem 294: 2021-2035, 2019.
21. Otto T and Sicinski P: Cell cycle proteins as promising targets in cancer therapy. Nat Rev Cancer 17: 93-115, 2017.
22. Asghar U, Witkiewicz AK, Turner NC and Knudsen ES: The history and future of targeting cyclin-dependent kinases in cancer therapy. Nat Rev Drug Discov 14: 130-146, 2015.
23. Thu KL, Soria-Bretones I, Mak TW and Cescon DW: Targeting the cell cycle in breast cancer: Towards the next phase. Cell Cycle 17: 1871-1885, 2018.
24. Taylor SC, Nadeau K, Abbasi M, Lachance C, Nguyen M and Fenrich J: The ultimate qPCR experiment: Producing publication quality, reproducible data the first time. Trends Biotechnol 37: 761-774, 2019.
25. Xu X, Nie J, Lu L, Du C, Meng F and Song D: LINC00337 promotes tumor angiogenesis in colorectal cancer by recruiting DNMT1, which suppresses the expression of CNN1. Cancer Gene Ther: Dec 16, 2020 (Online ahead of print).
26. Yatziv SL, Yudco O, Dickmann S and Devor M: Patterns of neural activity in the mouse brain: Wakefulness vs. General anesthesia. Neurosci Lett 735: 135212, 2020.
27. Washington MK, Berlin J, Branton PA, Burgart LJ, Carter DK, Compton CC, Frankel WL, Jessup JM, Kakar S, Minsky B, *et al*: Protocol for the examination of specimens from patients with carcinoma of the intrahepatic bile ducts. Arch Pathol Lab Med 134: e14-e18, 2010.
28. Hanahan D and Weinberg RA: The hallmarks of cancer. Cell 100: 57-70, 2000.
29. Drago JZ, Chandarlapaty S and Jhaveri K: Targeting apoptosis: A new paradigm for the treatment of estrogen receptor-positive breast cancer. Cancer Discov 9: 323-325, 2019.
30. Goldar S, Khaniani MS, Derakhshan SM and Baradaran B: Molecular mechanisms of apoptosis and roles in cancer development and treatment. Asian Pac J Cancer Prev 16: 2129-2144, 2015.
31. Mott JL, Bronk SF, Mesa RA, Kaufmann SH and Gores GJ: BH3-only protein mimetic obatoclax sensitizes cholangiocarcinoma cells to Apo2L/TRAIL-induced apoptosis. Mol Cancer Ther 7: 2339-2347, 2008.
32. Yang S, Meng J, Yang Y, Liu H, Wang C, Liu J, Zhang Y, Wang C and Xu H: A HSP60-targeting peptide for cell apoptosis imaging. Oncogenesis 5: e201, 2016.
33. Bene A and Chambers TC: p21 functions in a post-mitotic block checkpoint in the apoptotic response to vinblastine. Biochem Biophys Res Commun 380: 211-217, 2009.
34. Chen J: The cell-cycle arrest and apoptotic functions of p53 in tumor initiation and progression. Cold Spring Harb Perspect Med 6: a026104, 2016.
35. Snigdha S, Smith ED, Prieto GA and Cotman CW: Caspase-3 activation as a bifurcation point between plasticity and cell death. Neurosci Bull 28: 14-24, 2012.
36. Chakrabarty S and Kondratick L: Insulin-like growth factor binding protein-2 stimulates proliferation and activates multiple cascades of the mitogen-activated protein kinase pathways in NIH-OVCAR3 human epithelial ovarian cancer cells. Cancer Biol Ther 5: 189-197, 2006.
37. Zhong F, Yang J, Tong ZT, Chen LL, Fan LL, Wang F, Zha XL and Li J: Guggulsterone inhibits human cholangiocarcinoma Sk-ChA-1 and Mz-ChA-1 cell growth by inducing caspase-dependent apoptosis and downregulation of survivin and Bcl-2 expression. Oncol Lett 10: 1416-1422, 2015.
38. Chang Q, Liu ZR, Wang DY, Kumar M, Chen YB and Qin RY: Survivin expression induced by doxorubicin in cholangiocarcinoma. World J Gastroenterol 10: 415-418, 2004.
39. Endo T, Abe S, Seidlar HB, Nagaoka S, Takemura T, Utsuyama M, Kitagawa M and Hirokawa K: Expression of IAP family proteins in colon cancers from patients with different age groups. Cancer Immunol Immunother 53: 770-776, 2004.
40. Landskron G, De la Fuente M, Thuwajit P, Thuwajit C and Hermoso MA: Chronic inflammation and cytokines in the tumor microenvironment. J Immunol Res 2014: 149185, 2014.
41. Zhang Y and Weinberg RA: Epithelial-to-mesenchymal transition in cancer: Complexity and opportunities. Front Med 12: 361-373, 2018.
42. Singh M, Yelle N, Venugopal C and Singh SK: EMT: Mechanisms and therapeutic implications. Pharmacol Ther 182: 80-94, 2018.
43. Song X, Liu X, Wang H, Wang J, Qiao Y, Cigliano A, Utpatel K, Ribback S, Pilo MG, Serra M, *et al*: Combined CDK4/6 and Pan-mTOR inhibition is synergistic against intrahepatic cholangiocarcinoma. Clin Cancer Res 25: 403-413, 2019.
44. Samukawa E, Fujihara S, Oura K, Iwama H, Yamana Y, Tadokoro T, Chiyo T, Kobayashi K, Morishita A, Nakahara M, *et al*: Angiotensin receptor blocker telmisartan inhibits cell proliferation and tumor growth of cholangiocarcinoma through cell cycle arrest. Int J Oncol 51: 1674-1684, 2017.
45. Zhang Y, Ji G, Han S, Shao Z, Lu Z, Huo L, Zhang J, Yang R, Feng Q, Shen H, *et al*: Tip60 suppresses cholangiocarcinoma proliferation and metastasis via PI3k-AKT. Cell Physiol Biochem 50: 612-628, 2018.
46. Peng R, Zhang PF, Zhang C, Huang XY, Ding YB, Deng B, Bai DS and Xu YP: Elevated TRIM44 promotes intrahepatic cholangiocarcinoma progression by inducing cell EMT via MAPK signaling. Cancer Med 7: 796-808, 2018.
47. Wang Y, Liang Y, Yang G, Lan Y, Han J, Wang J, Yin D, Song R, Zheng T, Zhang S, *et al*: Tetraspanin 1 promotes epithelial-to-mesenchymal transition and metastasis of cholangiocarcinoma via PI3K/AKT signaling. J Exp Clin Cancer Res 37: 300, 2018.
48. Zhang MX, Gan W, Jing CY, Zheng SS, Yi Y, Zhang J, Xu X, Lin JJ, Zhang BH and Qiu SJ: S100A11 promotes cell proliferation via P38/MAPK signaling pathway in intrahepatic cholangiocarcinoma. Mol Carcinog 58: 19-30, 2019.